ORIGINAL ARTICLE

In vitro recovery of FIX clotting activity as a marker of highly functional hepatocytes in a hemophilia B iPSC model

Eléanor Luce[1,2] | Clara Steichen[1,2] | Mickaël Allouche[1,2] |
Antonietta Messina[1,2] | Jean-Marie Heslan[3] | Thierry Lambert[4] |
Anne Weber[1,2] | Tuan Huy Nguyen[3] | Olivier Christophe[5] |
Anne Dubart-Kupperschmitt[1,2]

[1]INSERM Université Paris-Saclay, Unité Mixte de Recherche 1193, Villejuif, France

[2]Féderation Hospitalo-Universitaire Hépatinov, Hôpital Paul Brousse, Villejuif, France

[3]INSERM Unité Mixte de Recherche 1064, CHU Hôtel Dieu, Nantes, France

[4]Centre de Référence pour le Traitement des Hémophiles, Hôpital de Bicêtre, France

[5]INSERM Unité Mixte de Recherche 1176, Hôpital de Bicêtre, Kremlin-Bicêtre, France

Correspondence
Eléanor Luce and Anne Dubart-Kupperschmitt, INSERM Université Paris-Saclay, Unité Mixte de Recherche (UMR_S) 1193, Villejuif, France.
Email: eleanor.luce@inserm.fr and anne.dubart@inserm.fr

Abstract

Background and Aims: Pluripotent stem cell–derived hepatocytes differentiated in monolayer culture are known to have more fetal than adult hepatocyte characteristics. If numerous studies tend to show that this immature phenotype might not necessarily be an obstacle to their use in transplantation, other applications such as drug screening, toxicological studies, or bioartificial livers are reliant on hepatocyte functionality and require full differentiation of hepatocytes. New technologies have been used to improve the differentiation process in recent years, usually evaluated by measuring the albumin production and CYP450 activity. Here we used the complex production and most importantly the activity of the coagulation factor IX (FIX) produced by mature hepatocytes to assess the differentiation of hemophilia B (HB) patient's induced pluripotent stem cells (iPSCs) in both monolayer culture and organoids.

Approach and Results: Indeed, HB is an X-linked monogenic disease due to an impaired activity of FIX synthesized by hepatocytes in the liver. We have developed an in vitro model of HB hepatocytes using iPSCs generated from fibroblasts of a severe HB patient. We used CRISPR/Cas9 technology to target the genomic insertion of a coagulation factor 9 minigene bearing the Padua mutation to enhance FIX activity. Noncorrected and corrected iPSCs were differentiated into hepatocytes under both two-dimensional and

Abbreviations: HU, Hounsfield unit; 2D, two-dimensional; 3D, three-dimensional; A1At, alpha-1 antitrypsin; AAV, adeno-associated virus; AFP, alfa-fetoprotein; ALB, albumin; APOA2, apolipoprotein A2; Bil-UGT, bilirubin-UDP-glucuronosyltransferase; BSEP, bile salt export pump; CK8, cytokeratin 8; corr-iHeps, corrected iHeps; CX32, connexin-32; CYP3A4, cytochrome P450 3A4; F9, coagulation factor 9; FIX, factor IX; GLA, gamma-carboxyglutamic acid; HB, hemophilia B; HB-iPSC, HB patient–specific iPSC; hiPSC, human-induced PSC; HLC, hepatocyte-like cell; HNF4α, hepatic nuclear factor 4α; iHep, induced hepatocyte; iPSC, induced pluripotent stem cell; MDR3, multidrug resistance protein 3; PAS, Periodic Acid Schiff; PHH, adult human hepatocyte; PSC, pluripotent stem cell; RPMI/B27, Roswell Park Memorial Institute 1640 medium with B27 serum-free supplement; SRB1, scavenger receptor B1; UDP, uridine diphosphoglucuronate; WT, wild-type; ZO-1, zona occludens 1.

----

three-dimensional differentiation protocols and deciphered the production of active FIX in vitro. Finally, we assessed the therapeutic efficacy of this approach in vivo using a mouse model of HB.

Conclusions: Functional FIX, whose post-translational modifications only occur in fully mature hepatocytes, was only produced in corrected iPSCs differentiated in organoids. Immunohistochemistry analyses of mouse livers indicated a good cell engraftment, and the FIX activity detected in the plasma of transplanted animals confirmed rescue of the bleeding phenotype.

INTRODUCTION

Hemophilia B (HB) is a genetic bleeding disorder caused by a mutation in the coagulation factor 9 (*F9*) gene, localized on the X chromosome (Xq27), and characterized by a reduced or absent functional clotting factor IX (FIX), a vitamin K–dependent serine protease synthesized in the liver by the hepatocytes. The clinical manifestations of HB depend on the severity of the disease, inversely related to the residual activity of FIX and accordingly classified as mild (5%-40% of normal), moderate (1%-5%), or severe (<1%). The clinical management of HB traditionally consists of the use of prophylactic treatments with FIX concentrates to reduce bleeding events and preserve joint function. However, this treatment presents certain limitations such as the considerable constraints represented by these repeated injections, affecting the daily life of patients, and its potential side effects such as the development of neutralizing antibodies.[1]

Two major treatment advances have recently emerged: (1) the use of recombinant FIX concentrates with a prolonged half-life[1] and (2) the gene therapy, which may enable a definitive cure for hemophilia. Indeed, HB is an ideal candidate for this strategy because it is a monogenic disease,[2] and the small size of FIX complementary DNA (cDNA; 1389bp) allows its insertion into most gene therapy vectors. Even if a modest increase in FIX activity (>1%) can substantially attenuate the bleeding risk for patients, the therapeutic efficacy of this approach can still be enhanced using a hyperfunctional FIX variant bearing the Padua mutation (R338L).[3] Very promising results have already been obtained with the gene therapy approach using adeno-associated virus (AAV) vectors in several clinical trials. However, not all patients will be eligible, and the systematic immune response against AAV capsids observed in the patients will impair a second vector infusion in case of decreasing efficacy.

The only curative treatment for HB is liver transplantation (LT), but due to the limited number of available organs, this approach is restricted to patients suffering from end-stage liver disease.[4] An alternative to LT might be hepatocyte transplantation,[5] because even 5%–10% of the FIX activity secreted by engrafted hepatocytes could considerably improve the prognosis and quality of life of patients suffering from severe HB. However, the availability of freshly isolated hepatocytes is limited because they cannot be amplified and they rapidly lose their liver-specific functions in vitro.[6] Other cell types can be used for cell therapy but have not proved particularly effective, such as (1) cadaveric hepatocytes, of poor quality and viability; (2) liver stem cells, little available and whose efficacy has not been demonstrated; or even (3) hepatocytes from fibroblast reprogramming, which display high levels of genetic and epigenetic variability.[7] Human pluripotent stem cells (PSCs) such as induced pluripotent stem cells (iPSCs)[8] have huge potential for cell therapy and regenerative medicine.[9] Culture conditions mimicking liver development with the sequential addition of specific cytokines and growth factors can drive the differentiation of PSCs into hepatocyte-like cells (HLCs) expressing specific liver markers such as hepatic nuclear factor 4α (HNF4α) or albumin and displaying hepatocyte-specific functions.[10,11] To date, a few studies have reported the generation of HB patient–specific iPSCs (HB-iPSCs)[12–16] and their differentiation into hepatocytes, but further characterization of the clotting FIX produced remains to be done.

CRISPR/Cas9 is now widely used as a cell editing approach. Insertion of a donor cassette into the *AAVS1* site (AAV integration site 1 within the first intron of the phosphatase 1 regulatory subunit 12C gene on chromosome 19) is known as a safe harbor region, where transgene expression from a chosen promoter does not cause insertional genotoxicity or oncogenic transformation and ensures its expression.[17] In the present study, we generated HB-iPSCs using fibroblasts from a severe HB patient with the g.31280 G>A (c.1297G>A, p.E433K) mutation, leading to the production of an inactive FIX protein, and established a human HB model using hepatocytes differentiated from these HB-iPSCs (HB-iHeps). As a cell/gene therapy approach, we used the CRISPR/Cas9 technology to insert a correction cassette, which included a *F9* minigene-encoding FIX

bearing the Padua mutation (p.R384L) to enhance FIX specific activity,[3] under the control of the hepatic-specific apolipoprotein A2 (*APOA2*) promoter, into the *AAVS1* site of HB-iPSCs.

After differentiation into hepatocytes in a conventional 2D culture system, noncorrected (HB-iHeps) and corrected (corr-iHeps) cells showed an incomplete maturation, also observed by others.[18] We therefore set up the culture conditions for a differentiation in three dimensions (3D) and were able to measure FIX activity in vitro in corr-iHeps, confirming an improved cell differentiation in 3D compared with two dimensions (2D). Finally, we confirmed our approach of cell/gene therapy in a mouse model of HB (*F9*KO) after intrahepatic transplantation of corr-iHeps.

MATERIALS AND METHODS

Correction of the genetic defect in HB-iPSCs using CRISPR/Cas9 technology

HB-iPSCs were cultured under feeder-free conditions on Geltrex-coated culture dishes (Gibco) for a few passages in StemMACS iPS-Brew XF medium (Miltenyi Biotec), with 1% penicillin-streptomycin (Gibco). On the day of transfection, the cells were treated with 10 μM Y-27632 (Stemcell Technologies) 4 hours before detachment with accutase (Gibco). A total of 2.5×10^6 cells were nucleofected using the Amaxa Nucleofector device (Lonza) with three plasmids harboring the single-guide RNA AAVS1 targeting sequence (GGGGCCACTAGGGACAGGAT), the spCas9 endonuclease, and a donor cassette containing a *F9* minigene with the Padua mutation (g.31134 G>T, p.R384L) under the control of the human *APOA2* promotor cloned into the pZDonor-AAVS1 puromycin vector (Sigma). Corrected clones were then selected by gradually increasing the puromycin concentrations (0.5–2 μg/ml; Sigma) and clonal picking.

Hepatocyte differentiation of human-induced PSCs

The hepatocyte differentiation of human-induced PSCs (hiPSCs) was driven by successive additions of specific growth factors mimicking signals from the micro-environment during liver development. Briefly, 3 days before collection for seeding, hiPSCs were treated with 100 ng/ml Wnt3a (R&D). The cells were then collected after treatment for 5 minutes with trypsin-EDTA (0.5%) (Gibco) at 37°C and then incubated for 20 min on a gelatin-coated dish to remove the MEF feeder cells. The cells were then seeded onto six-well plates (Corning) precoated with 0.1% porcine gelatin (Sigma) at 40,000 cells/cm² in RPMI/B27 (Roswell Park Memorial Institute

1640 medium [Gibco] with B27 serum-free supplement [Life technologies]), 1% nonessential amino acids, 1% L-glutamine, and 1% penicillin-streptomycin (all from Gibco)), supplemented with 10 nM Y-27632 (Stemcell Technologies), 100 ng/ml Activin A (CellGenix), and 3 nM CHIR-99021 (Stemcell Technologies). After 24 h, the medium was removed and the cells were cultured in RPMI/B27 with 100 ng/ml Activin A alone for 4 days. They were then cultured for 3 days in RPMI/B27 with 10 ng/ml BMP4 (R&D Systems) and 10 ng/ml FGF2 (CellGenix), and 2 further days in methionine-deprived RPMI (Gibco) with 20 ng/ml HGF (Peprotech), 30 ng/ml FGF4 (Peprotech), and 10 ng/ml EGF (Peprotech); they then reached the hepatoblast stage, the bipotent progenitors of hepatocytes and cholangiocytes.

The hepatoblasts were harvested using accutase (Gibco) and seeded onto six-well collagen I-coated plates in plating medium (RPMI/B27, 10% fetal bovine serum [Gibco], 1% bovine serum albumin [BSA; Sigma], 20 ng/ml HGF) for 4 hours to enable 2D hepatocyte differentiation.

For 3D hepatocyte differentiation, six-well plates were prepared as described.[19] Briefly, sterilized powdered Ultrapure agarose (Life Technologies) was dissolved (2% wt/vol) by heating in sterile water. The liquid agarose solution was added to one well of a six-well plate and left to solidify at room temperature while cylindrical microwells of 1-mm diameter and depth were formed using a home-made silicone mold. After cooling, the molds were lifted from the agarose gel and a single-cell suspension of 1.4×10^6 cells/ml was added to the wells. After 30 min, the cells settled into the bottoms of the microwells and formed micro-aggregates within a few hours.

The following steps were then applied to both 2D and 3D hepatocyte differentiation. The culture medium was replenished and changed every day for 4 days with RPMI-1640 medium plus 1% insulin-transferrin-selenium (Gibco), 0.1% BSA, 4.5 mM nicotinamide, 0.1 nM zinc sulfate heptahydrate, and 6×10^{-4}M ascorbic acid (all from Sigma), supplemented with 20 ng/ml HGF, 10 ng/ml EGF, 100 nM dexamethasone (Dex; Sigma), and 20 ng/ml oncostatin M (Peprotech). Finally, the cells were kept in culture until the end of differentiation in the same medium supplemented with 5×10^{-8} M 3,3′,5-triiodo-L-thyroxine (Sigma), 20 ng/ml HGF, 100 nM Dex, 0,5 nM Compound E (Santa Cruz), 5 nM SB431452 (Tocris), and 10 ng/ml vitamin K1 (Roche).

Immunoprecipitation and western blot analyses

Total cellular proteins were extracted using radio immunoprecipitation assay lysis buffer (50 mM Tris-HCl, 150 mM NaCl, 1% Triton X-100, 1% sodium deoxycholate, 0.1% sodium dodecyl sulfate [SDS], 2 mM

ethylene diamine tetraacetic acid [EDTA], all from Sigma) with the addition of a protease inhibitor cocktail (Roche). Protein concentrations were determined using a DC Protein Assay (Biorad) according to the manufacturer's instructions. A total of 300 µg of total proteins were used for immunoprecipitation using Protein G Sepharose Fast Flow beads (Sigma) and an anti-human FIX antibody (Affinity Biologicals) (Table S1). Proteins were resolved on a 12% acrylamide-SDS gel, transferred to a Hybond Amersham polyvinylidene fluoride membrane (GE Healthcare), and probed overnight at 4°C with primary antibodies after saturation in PBS (0.1% Tween 20 [Sigma]) and 5% dry milk. The membrane was then incubated for 1 hour at room temperature with secondary specific horseradish peroxidase–conjugated antibody, and the specific bands were finally visualized with the Clarity Western Enhanced Chemiluminescence Reagent substrate kit (Biorad). Images were generated using a Fusion solo camera and its software (Vilber).

FIX protein expression was also studied using a WES separation module (Proteinsimple) following the manufacturer's instructions. Briefly, total cellular proteins were mixed with Fluorescent Master Mix (PS-ST01 Wes) and denatured at high temperature. A rabbit anti-human FIX antibody (DAKO) was used as the primary antibody, and the plate was loaded into the WES machine.

FIX activity

FIX chromogenic activity was determined using the Biophen FIX-assay kit (Hyphen) following the manufacturer's instructions.

Transplantation of corrected HB-iHeps into a mouse model of HB

All animal studies were carried out in accordance with French guidelines regarding the care and use of experimental animals and approved by the French Ethics Committee C2EA-26 for animal experiments under number 509 1 2015062215414016. HB mouse farming (Jackson Laboratory, strain name B6; 129P2-F9tm1Dws/J[20]) was established under pathogen-free conditions, and newborn mice from the mating of F9KO heterozygous female and F9KO male mice were used for this study. Forty-eight hours after birth, each newborn mouse from the same litter received a transcutaneous injection into the liver using a 29-gauge needle of both 10^5-corrected HB-iPSCs at day 11 of hepatocyte differentiation and 1U of recombinant FIX (BeneFIX; Pfizer), to ensure the survival of hemophilic mice. After 2 weeks, the mice were sacrificed and genotyped by PCR using the primers listed in Table S2. The livers and plasma were collected for further study.

See Supporting Information for additional materials and methods.

RESULTS

Use of patient-specific iPSCs for the disease modeling of HB

Using a polycistronic lentivector encoding the four Yamanaka factors (rLV-EF1-OCT4-SOX2-KLF4-cMYC, Vectalys), we reprogrammed skin fibroblasts from a patient with severe HB (FIX c < 1%; IXAg 67%) carrying a g.31280 G>A (c.1297G>A, p.E433K) mutation. The full characterization of one iPSC line (HB-iPSCs) by immunostaining (Figure S1A) and flow cytometry analysis (Figure S1B) revealed the expression of endogenous stem cell markers such as OCT4, NANOG, SSEA4, TRA-1-80, and TRA-1-60. Real-time PCR analyses of cells derived from randomly formed embryoid bodies in vitro highlighted the expression of markers from the three germ layers (Figure S1C). A few weeks after the injection of HB-iPSCs into NOD-SCID mice, the teratomas produced contained multiple derivatives of the three germ layers (Figure S1D), attesting to the pluripotency of HB-iPSCs. The karyotype of the iPSCs was normal (Figure S1E), and DNA sequencing confirmed the presence of the patient's mutation in the HB-iPSCs (Figure S1F).

Genetic correction of HB-iPSCs using CRISPR/Cas9 technology

To correct the phenotypic defect in the cells, we used the CRISPR/Cas9 cell editing approach to insert a therapeutic cassette into the safe harbor AAVS1 site. This therapeutic cassette included a F9 minigene, bearing the Padua mutation (g.31134 G>T, p.R384L), under the control of the hepatic-specific promoter of APOA2 (Figure 1A). After treatment with increasing doses of puromycin, 70 resistant colonies were picked and individually expanded. The genomic DNA of each of these clones was further analyzed by PCR using primers spanning the 5′ and 3′ homology arms; this revealed an accurate integration of the cassette in 21% of the puromycin-resistant clones (15 of 70) (Figure 1B). An intact endogenous AAVS1 allele was detected in all the tested clones, indicating monoallellic integration of the cassette (Figure 1C). Sequencing of the homologous recombination 5′ and 3′ regions, and of a part of the F9 minigene, confirmed their genetic stability during the gene editing process (data not shown) and the presence of the Padua mutation in the corrected cells (Figure 1D). We also confirmed the normality of the
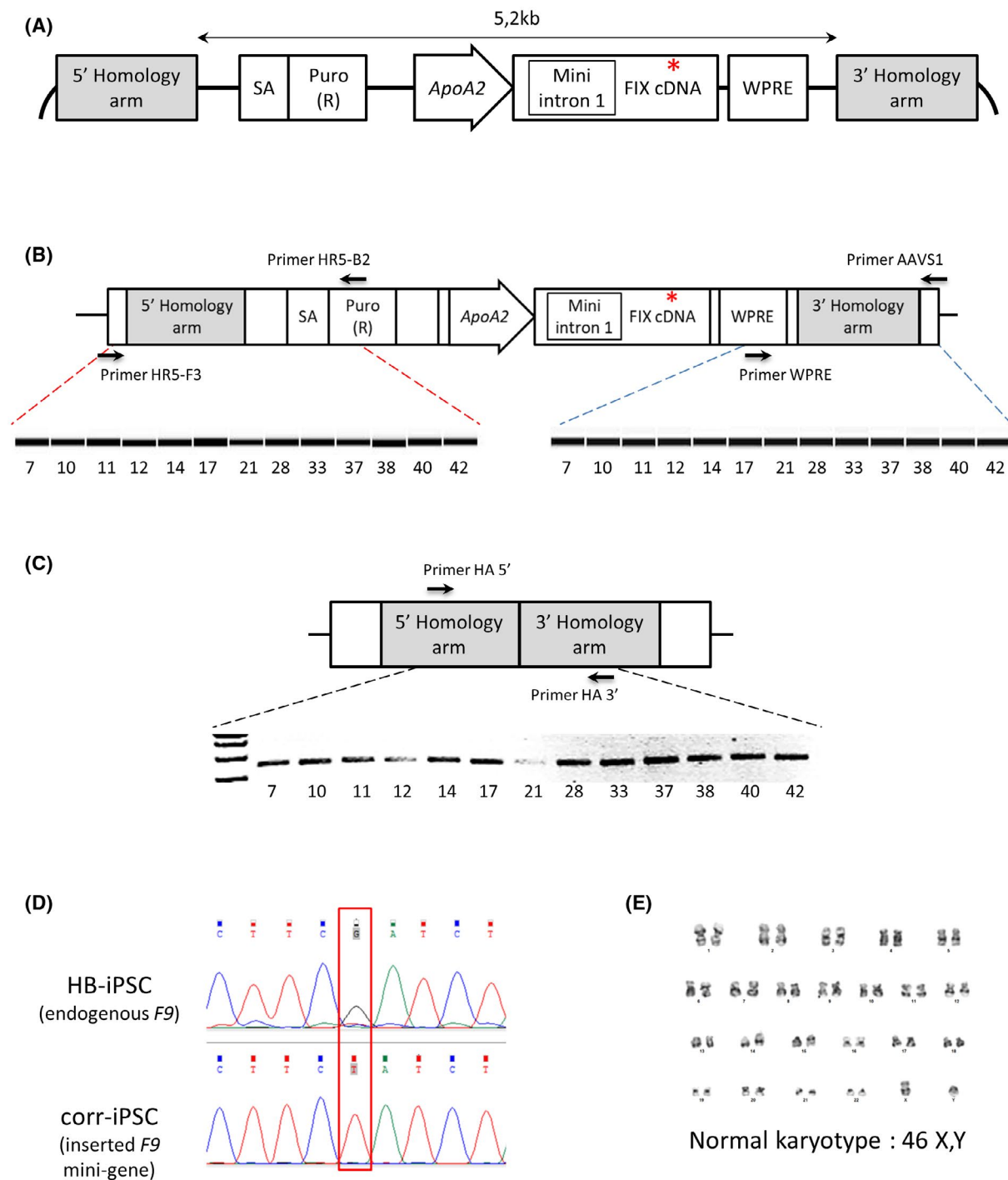
FIGURE 1 Genetic correction of hemophilia B patient–specific induced pluripotent stem cells (HB-iPSCs) using CRIPSR/Cas9 technology. (A) Schematic representation of the therapeutic cassette in the adeno-associated virus (AAV) S1 SA-2A-puro-pA donor plasmid containing homology sequences to the sequence of the targeted *AAVS1* site. The expression cassette includes the apolipoprotein A2 (*APOA2*) promoter that drives the expression of a coagulation factor 9 (*F9*) minigene bearing the Padua mutation (red star) to enhance factor IX (FIX)–specific activity, and a puromycin resistance sequence for the selection of corrected clones (Puro). (B) Confirmation of correct insertion of the cassette at the targeted site. The PCR analysis using primers flanking homologous recombination regions evidenced amplification of the expected DNA fragments. (C) PCR analysis of the *AAVS1* targeted site, showing the absence of integration of the therapeutic cassette in one of the alleles. (D) Example of confirmation of the presence of the Padua mutation in corrected clones by sequencing a portion of the *F9* minigene. (E) Confirmation of the normality of the karyotype in the corrected clone selected for hepatocyte differentiation. Abbreviations: cDNA, complementary DNA; corr-iHeps, corrected iHeps; iHeps, induced hepatocytes; SA, splice acceptor site; and WPRE, Woodchuck hepatitis virus post-transcriptional regulatory element that improves mRNA nuclear export and hence protein expression
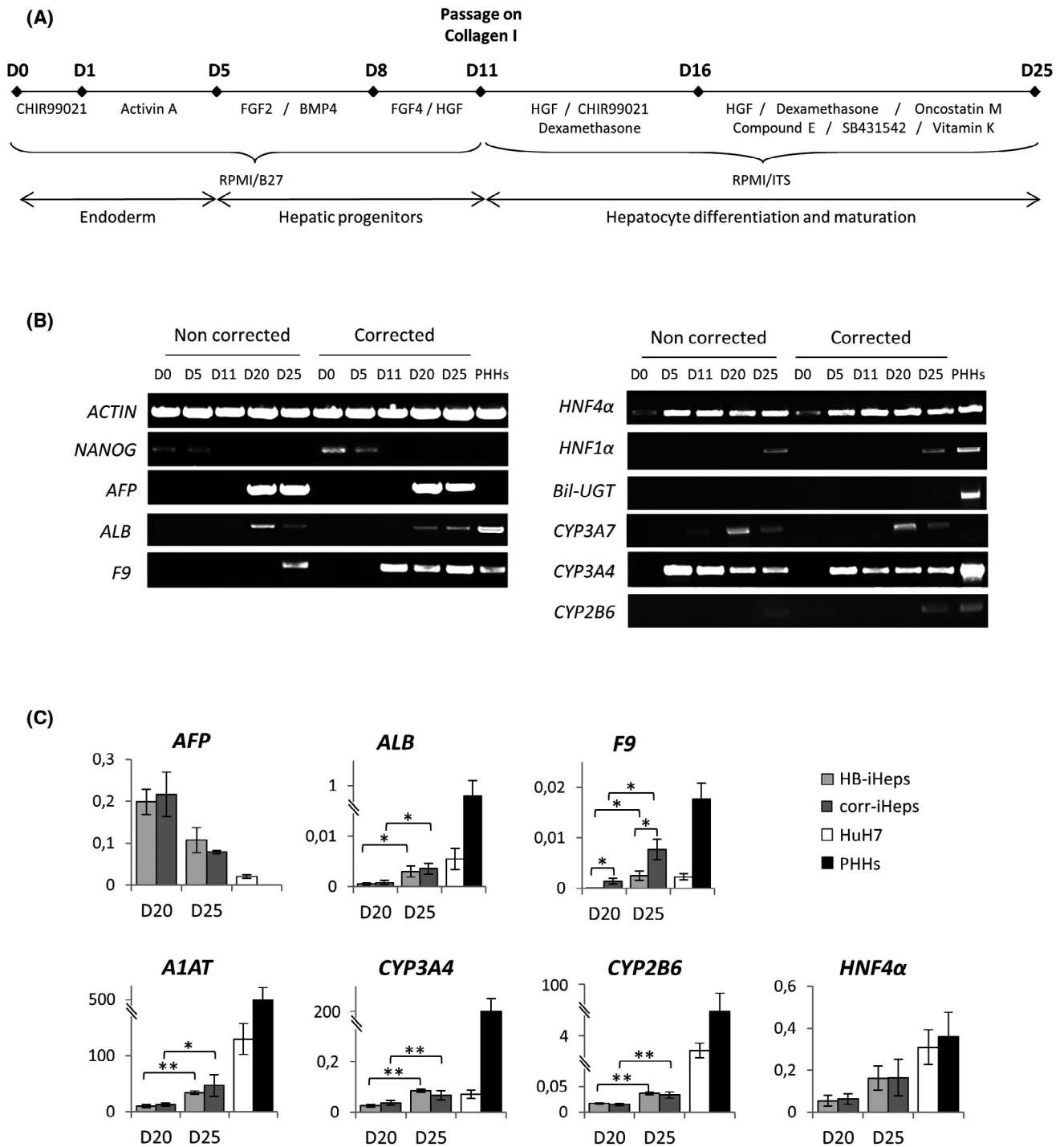
FIGURE 2 Hepatocyte differentiation of corrected and noncorrected HB-iPSCs under two-dimensional (2D) conditions. (A) Schematic representation of the protocol used for human-induced PSC (hiPSC) differentiation into hepatocytes. (B) Real-time PCR analyses show the expression pattern during hepatocyte differentiation of both corrected and noncorrected cells at days 0, 5, 11, 20, and 25. Cryopreserved adult human hepatocytes (PHHs) were used as controls. (C) Relative quantification of hepatic mRNA levels at days 20 and 25 of the differentiation protocol by quantitative real-time PCR in HB-iHeps and corr-iHeps. Gene-expression levels were measured in triplicates and normalized using *RPL13a* expression. PHHs and HuH7 cells were used as controls. Results are expressed as mean ± SD (*n* = 3). Statistical significance was determined using the Student *t* test; *p < 0.05, **p < 0.01. Abbreviations: *A1AT*, α1-antitrypsin; *AFP*, alfa-fetoprotein; *ALB*, albumin; *Bil-UGT*, bilirubin-UDP-glucuronosyltransferase; BMP4, bone morphogenetic protein 4; *CYP3A4/3A7/2B6*, cytochrome P450 3A4*/3A7/2B6*; *HNF4α/1α*, hepatocyte nuclear factor 4α/1α; and RPMI, Roswell Park Memorial Institute 1640 medium

karyotype (Figure 1E) and selected a representative clone (corr-iPSCs) for further experiments.

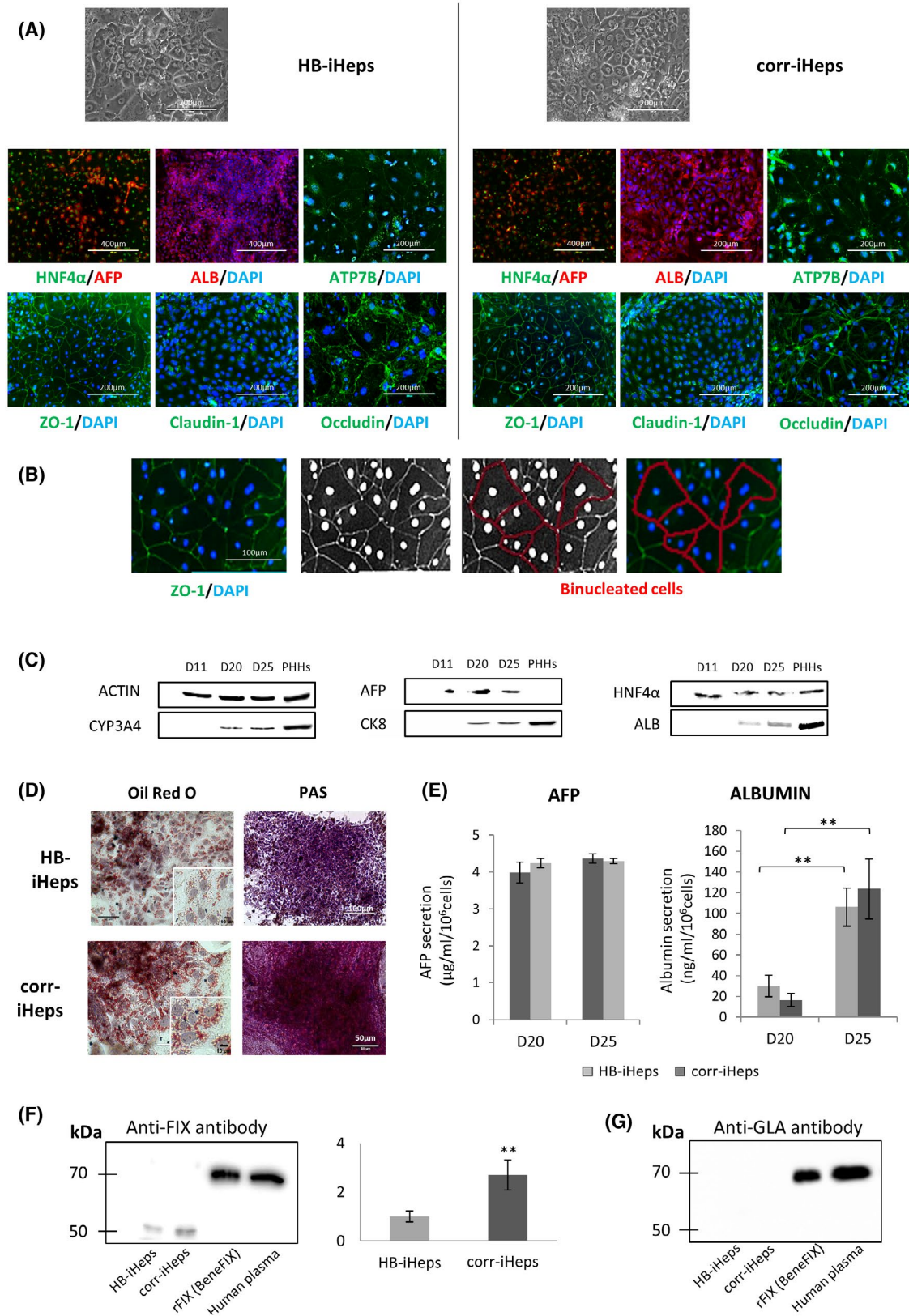## Differentiation of HB-iPSCs and corr-iPSCs into hepatocytes

Based on previously published protocols,[21,22] we developed chemically defined conditions and sequential addition of growth factors mimicking major steps in normal development and liver organogenesis to differentiate both noncorrected and corrected iPSCs into hepatocyte-like cells (HB-iHeps and corr-iHeps, respectively) (Figure 2A). Undifferentiated iPSCs were incubated for 24 hours with CHIR99021, an inhibitor of the glycogen synthase kinase 3β, known to promote the differentiation of embryonic stem cells toward primitive streak, mesoderm and definitive endoderm.[23] The cells were subsequently incubated with a high concentration of Activin A to induce a definitive endoderm phenotype, leading to the expression of specific markers such as the transcription factor GATA Binding Protein 4 (GATA4) and chemokine (C-X-C motif) receptor 4 (CXCR4) at day 5 of differentiation (Figure S2A). After specification of the definitive endoderm, the cells differentiated into bipotent hepatic progenitors, known as hepatoblasts, which at day 11 expressed HNF4α and biliary marker cytokeratin 19 (CK19) as well as alpha-1 antitrypsin (A1AT), forkhead box A2 (FOXA2), and epithelial cell adhesion molecule (EPCAM) (Figure S2B). Cells were passaged at day 11 on a collagen matrix and treated with dexamethasone, HGF, and CHIR99021 to promote their proliferation. Quantitative real-time PCR showed the expression of *F9* mRNA specific to the inserted cassette in differentiating corr-iPSCs starting at day 5 and due to the *APOA2* promoter (Figure S2C). We finally treated the cells with inhibitors of both the Notch and TGFβ pathways, which are known to be involved in cholangiocyte lineage specification, using Compound E and SB431542, respectively. We also treated the cells with vitamin K1, as 1% of the total proteins synthesized by the liver and secreted into the plasma, including FIX, are vitamin K-dependent.[24]

Gene-expression analysis performed at each step of the protocol (i.e., definitive endoderm, hepatic progenitors, and iHeps) indicated the gradual silencing of pluripotency markers such as *NANOG*, and the appearance of hepatic markers such as alfa-fetoprotein (*AFP*), *HNF4α*, *HNF1α*, albumin (*ALB*), cytochrome P450 3A4, 3A7 and 2B6 (*CYP3A4/3A7/2B6*), bilirubin– uridine diphosphoglucuronate (UDP)–glucuronosyltransferase (*Bil-UGT*), and *F9* (Figure 2B). Hepatic mRNA were quantified by quantitative real-time PCR, confirming the decrease of *AFP* mRNA level between days 20 and 25 and the significant increase of *albumin*, *A1AT*, and *CYP3A4/3A7/2B6*. Quantitative analysis of *F9* mRNA showed a 3.5-fold higher abundance of *F9* mRNA in corr-iHeps than in HB-iHeps at day 25, using primers that recognize both endogenous and transgene expression (Figure 2C).

At the end of the differentiation, the morphology of both corr-iHeps and HB-iHeps closely resembled that of primary human hepatocytes, which are polygonal in shape. As assessed by immunostaining analyzes, most of the cells expressed hepatocyte-specific markers such as HNF4α, AFP, ALB, and ATP7B (Figure 3A). Furthermore, differentiated cells exhibited signs of epithelial polarity, as shown by the lateral membrane staining of zona occludens 1 (ZO-1), occludin and claudin-1, which are three tight junction proteins. The staining of both cell nuclei and membranes highlighted the presence of binucleated cells, a characteristic feature of mature hepatocytes (Figure 3B). Protein analysis by western blot confirmed the expression of hepatic markers such as AFP, HNF4α, albumin, CYP3A4, cytokeratin 8 (CK8), and HNF4α in differentiated cells (Figure 3C). Some hepatocyte functions were also visualized, such as lipid and glycogen storage using Periodic Acid Schiff (PAS) and Oil Red O staining, respectively (Figure 3D). AFP secretion measured by ELISA remains stable from day 20 to 25 in both HB-iHeps and corr-iHeps, while secretion of albumin significantly increased (Figure 3E), thus indicating cell maturation during the final days of differentiation.

To further study the expression of FIX in differentiated iHeps, western blot analyses were performed on

FIGURE 3 Characterization of HB-iHeps and corr-iHeps differentiated under 2D conditions. (A) Morphologies of HB-iHeps and corr-iHeps at day 25 of differentiation and immunostaining of hepatocyte markers. Nuclei were counterstained with 4′,6-diamidino-2-phenylindole (DAPI). (B) Immunostaining of hepatocyte nuclei and membranes and image processing showing binucleated cells. (C) Western blot analysis of hepatic proteins at days 11, 20, and 25 of the differentiation protocol in HB-iHeps and corr-iHeps. Cryopreserved adult human hepatocytes (PHHs) have been used as internal control and actin as loading control. (D) Oil Red O and Periodic Acid Schiff (PAS) staining of HB-iHeps and corr-iHeps, evidencing lipid and glycogen storage, respectively. (E) Determination of AFP and albumin secretion by HB-iHeps and corr-iHeps using ELISA at days 20 and 25. Results are expressed as mean ± SD ($n \geq 3$). Statistical significance was determined using the Student *t* test; **$p < 0.01$. (F) Western blot analysis of immunoprecipitated FIX from HB-iHep and corr-iHep cell extracts at day 25 of differentiation. Recombinant FIX (rFIX; BeneFIX) and human plasma were used as controls. The FIX bands obtained in both differentiated clones were quantified using ImageJ software, where the FIX band in HB-iHeps was set arbitrarily at 1. Results are expressed as mean ± SD ($n = 3$). Statistical significance was determined using the Student *t* test; **$p < 0.01$. (G) Western blot analysis of immunoprecipitated FIX from HB-iHep and corr-iHep cell extracts at day 25 of differentiation using antibody directed against the gamma-carboxyglutamic acid (GLA) domain of the post-translationally modified protein. rFIX and human plasma were used as controls. Abbreviations: ATP7B, copper-transporting P-type ATPase; CK8, cytokeratin 8; and ZO-1, zonula occludens-1

(A) HB-iHeps / corr-iHeps

HNF4α/AFP   ALB/DAPI   ATP7B/DAPI

ZO-1/DAPI   Claudin-1/DAPI   Occludin/DAPI

(B)

ZO-1/DAPI   Binucleated cells

(C)

	D11	D20	D25	PHHs
ACTIN				
CYP3A4				

	D11	D20	D25	PHHs
AFP				
CK8				

	D11	D20	D25	PHHs
HNF4α				
ALB				

(D)   Oil Red O   PAS

HB-iHeps

corr-iHeps

(E)   AFP   ALBUMIN

AFP secretion (µg/ml/10^{6}cells)

Albumin secretion (ng/ml/10^{6}cells)

D20   D25

□ HB-iHeps   ■ corr-iHeps

(F) Anti-FIX antibody

kDa
70
50

HB-iHeps   corr-iHeps   rFIX (BeneFIX)   Human plasma

**

HB-iHeps   corr-iHeps

(G) Anti-GLA antibody

kDa
70
50

HB-iHeps   corr-iHeps   rFIX (BeneFIX)   Human plasma

immunoprecipitated cell lysates. As shown on Figure 3F, we observed a 2.7-fold higher production of FIX in corr-iHeps than in HB-iHeps. However, the molecular weight of the FIX protein present in the differentiated cells was of 50 kDa, corresponding to the inactive form of the protein, whereas recombinant and plasmatic FIX were both of approximately 70 kDa due to post-translational modifications. Hybridization of the western blot with an

antibody directed against the gamma-carboxyglutamic acid (GLA) domain of the protein evidenced an absence of γ-carboxylation of this domain (Figure 3G). The lack of proper FIX post-translational modifications suggests that differentiated iHeps are not fully mature. This incomplete maturation led us to investigate the capacity of a 3D culture to improve the differentiation stage of iHeps and to result in the production of a correctly processed FIX.[25]

Generation of 3D organoids

Hepatoblasts were seeded at day 11 into inert agarose wells to self-assemble in aggregates and then organoids, while the differentiation protocol used up to day 25–30 was similar to the one described in Figure 2A.

As for the 2D differentiation protocol, gene-expression analysis indicated the gradual silencing of pluripotency markers such as *NANOG*, and the appearance of hepatic markers such as *AFP*, *HNF4α*, *HNF1α*, *ALB*, *CYP3A4/3A7/2B6*, *Bil-UGT*, and *F9* (Figure 4A). Hepatic mRNA were quantified by quantitative real-time PCR, confirming the decrease of *AFP* mRNA level between days 20 and 25 and the significant increase of *albumin*, *A1AT*, and *CYP3A4/3A7/2B6* (Figure 4B). We also observed a 4-fold higher expression of *F9* mRNA in corr-iHeps at day 25 of hepatocyte differentiation when compared with HB-iHeps, using primers that recognized both endogenous and transgene expression. However, a comparison between 2D and 3D differentiated cells showed an 11-fold increase in *ALB* mRNA for HB-iHeps and a 14-fold increase for corr-iHeps at day 25. Moreover, a significant improvement in hepatocyte differentiation efficiency and cell maturation was indicated by a 50-fold increase in the *F9* mRNA level for HB-iHeps and an 80-fold increase for corr-iHeps.
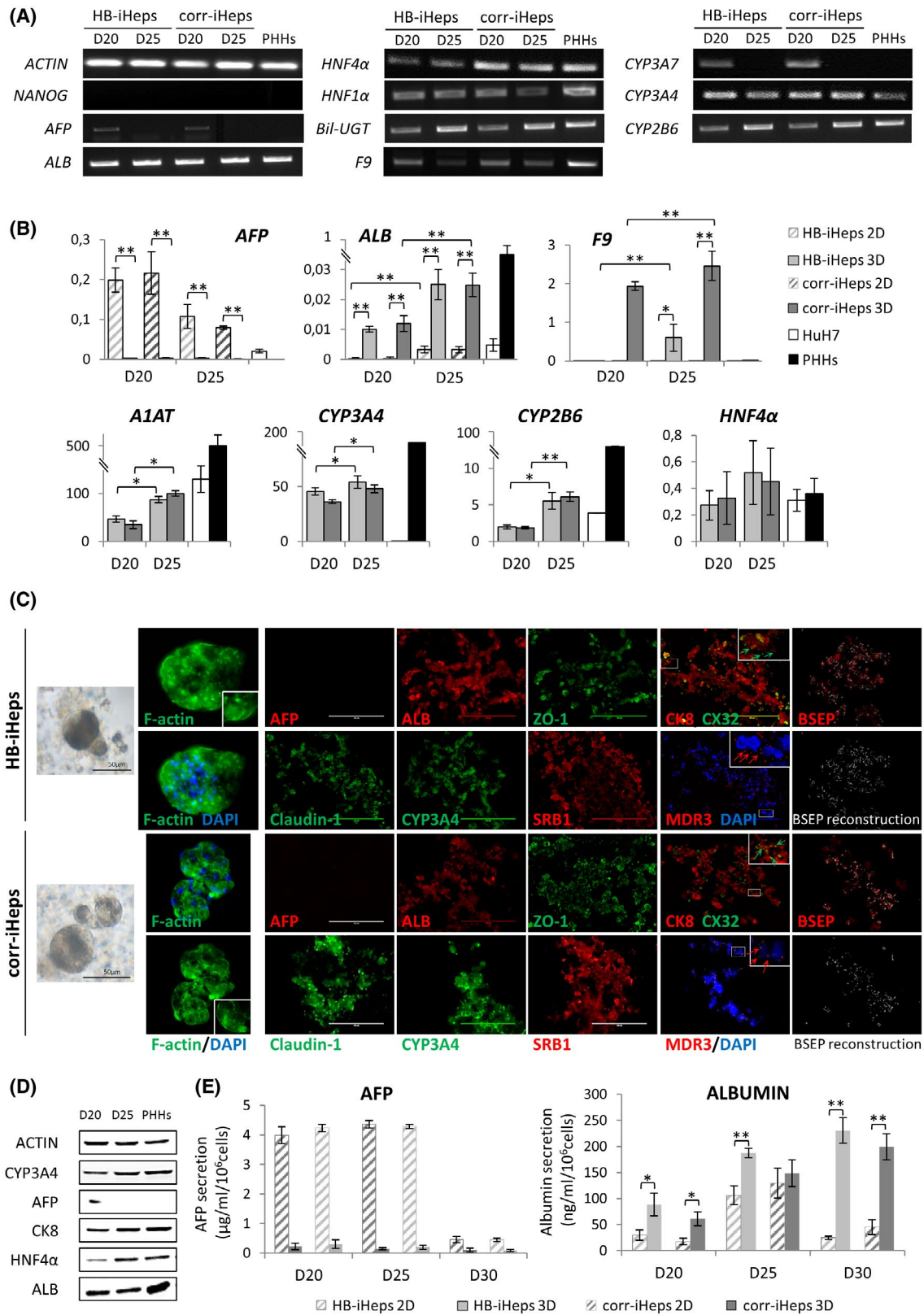
The organoids of both HB-iHeps and corr-iHeps were round in shape and of the same size (about 50 µm in diameter) (Figure 4). They expressed hepatocyte markers such as albumin, ZO-1, and claudin-1 (Figure 4C). Immunostainings also highlighted the improvement in cell maturation when compared with the 2D protocol, as reflected by the disappearance of AFP labeling at day 25 in 3D organoids. Moreover, the cells expressed mature hepatocyte markers such as one of the major cytochromes P450 (CYP3A4), the high-density lipoprotein receptor called scavenger receptor B1 (SRB1), hepatocyte-specific CK8, and the connexin-32 (CX32) involved in Gap junction–mediated cell–cell interactions during hepatocyte maturation.[26] The differentiated cells acquired complex polarization under 3D conditions, which was highlighted at the biliary pole of the hepatocytes by the expression of multidrug resistance protein 3 (MDR3), one of the major ABC transporters responsible for phospholipid transport, as well as the bile salt export pump (BSEP), an efflux transporter that plays an important role in eliminating bile salts from hepatocytes into the bile canaliculi. Protein analysis by western blot confirmed the appearance of hepatic markers such as AFP, ALB, CYP3A4, CK8, and HNF4α (Figure 4D). The 3D differentiated cells were also able to store lipids and glycogen, as shown by Oil Red O and PAS staining, respectively (Figure S3A).

Excretion of the fluorescent dye CDFDA (5[6]-Carboxy-2′,7′-dichlorofluorescein diacetate) into the bile canaliculi of differentiated cells, which implies biliary efflux through multidrug resistance protein transporter 2 (MRP2), confirmed the functionality of the bile canaliculi between polarized differentiated cells (Figure S3B). Finally, both HB-iHeps and corr-iHeps differentiated under 3D conditions were able to uptake indocyanine green (ICG) within 4 hours through the organic anion transporting polypeptide (OATP1B1) and Na(+)/taurocholate cotransporter polypeptide (NTCP), and then release it into bile canaliculi across MDR2, thus highlighting efficient metabolic functions from phases 1 to 3 (Figure S3C).

Analysis of the supernatants of 3D differentiated cells revealed a reduction in AFP secretion, whereas albumin secretion continued to increase between day 20 and day 30, thus highlighting the continuous differentiation of hepatocytes (Figure 4E). Moreover, a comparison between 2D and 3D differentiation showed significantly higher albumin production at day 30, thus confirming the gradual acquisition of an adult hepatocyte phenotype under our 3D culture system.

FIGURE 4   Characterization of HB-iHeps and corr-iHeps differentiated in organoids. (A) Real-time PCR analyses show the expression pattern during hepatocyte differentiation of both corrected and noncorrected cells in organoids at days 20 and 25. Cryopreserved PHHs were used as controls. (B) Relative quantification of hepatic mRNA levels determined by quantitative real-time PCR in HB-iHeps and corr-iHeps at days 20 and 25 of the three-dimensional (3D) differentiation protocol. Gene-expression levels were measured in triplicate and normalized according to *RPL13a* expression. PHHs and HuH7 cells were used as controls. Results are expressed as mean ± SD (n = 3). Statistical significance was determined using the Student *t* test; *$p < 0.05$, **$p < 0.01$. (C) Morphology and F-actin staining of whole organoids of HB-iHeps and corr-iHeps at day 25 and immunostaining of HB-iHeps and corr-iHeps at day 25 of the differentiation protocol on cryosections of organoids embedded in optimal cutting temperature (OCT) compound. Scale bars represent 100 µm. The computational 3D reconstruction of BSEP was processed using ImageJ plugins.[36] (D) Western blot analysis of hepatic proteins at days 20 and 25 of the 3D differentiation protocol in HB-iHeps and corr-iHeps. PHHs have been used as internal control and actin as loading control. (E) AFP and albumin secretion by HB-iHeps and corr-iHeps was determined by ELISA at days 20 and 30. Results are expressed as mean ± SD ($n \geq 3$). Statistical significance was determined using the Student *t* test; *$p < 0.05$, **$p < 0.01$. Abbreviations: BSEP: bile salt export pump; CX32, connexin-32/gap junction protein β1; MDR3, multidrug resistance protein 3; and SRB1, scavenger receptor class B member 1

(A) RT-PCR panels: HB-iHeps (D20, D25), corr-iHeps (D20, D25), PHHs for ACTIN, NANOG, AFP, ALB; HNF4α, HNF1α, Bil-UGT, F9; CYP3A7, CYP3A4, CYP2B6.

(B) Gene expression bar charts: AFP, ALB, F9, A1AT, CYP3A4, CYP2B6, HNF4α. Legend: HB-iHeps 2D, HB-iHeps 3D, corr-iHeps 2D, corr-iHeps 3D, HuH7, PHHs.

(C) Immunofluorescence images for HB-iHeps and corr-iHeps: F-actin, F-actin/DAPI, AFP, ALB, ZO-1, Claudin-1, CYP3A4, SRB1, CK8 CX32, MDR3/DAPI, BSEP, BSEP reconstruction.

(D) Western blot: ACTIN, CYP3A4, AFP, CK8, HNF4α, ALB (D20, D25, PHHs).

(E) AFP and ALBUMIN secretion bar charts. Legend: HB-iHeps 2D, HB-iHeps 3D, corr-iHeps 2D, corr-iHeps 3D.

Genetic correction rescues the HB phenotype in vitro

As revealed by immunofluorescence at day 30 of 3D differentiation, both HB-iHeps and corr-iHeps expressed FIX (Figure 5A). Of note, the g.31280 G>A mutation impaired FIX activity but not FIX synthesis by hepatocytes. Automated WES analysis performed on immunoprecipitated cell lysates of 2D-differentiated and 3D-differentiated cells, from the same hepatoblast

population, indicated different FIX profiles of migration (Figure 5B). Indeed, this analysis confirmed the low molecular weight of the FIX protein present in HB-iHeps and corr-iHeps differentiated in 2D (50 kDa). However, the FIX protein expressed after 3D differentiation reached almost 70 kDa, as observed for the reco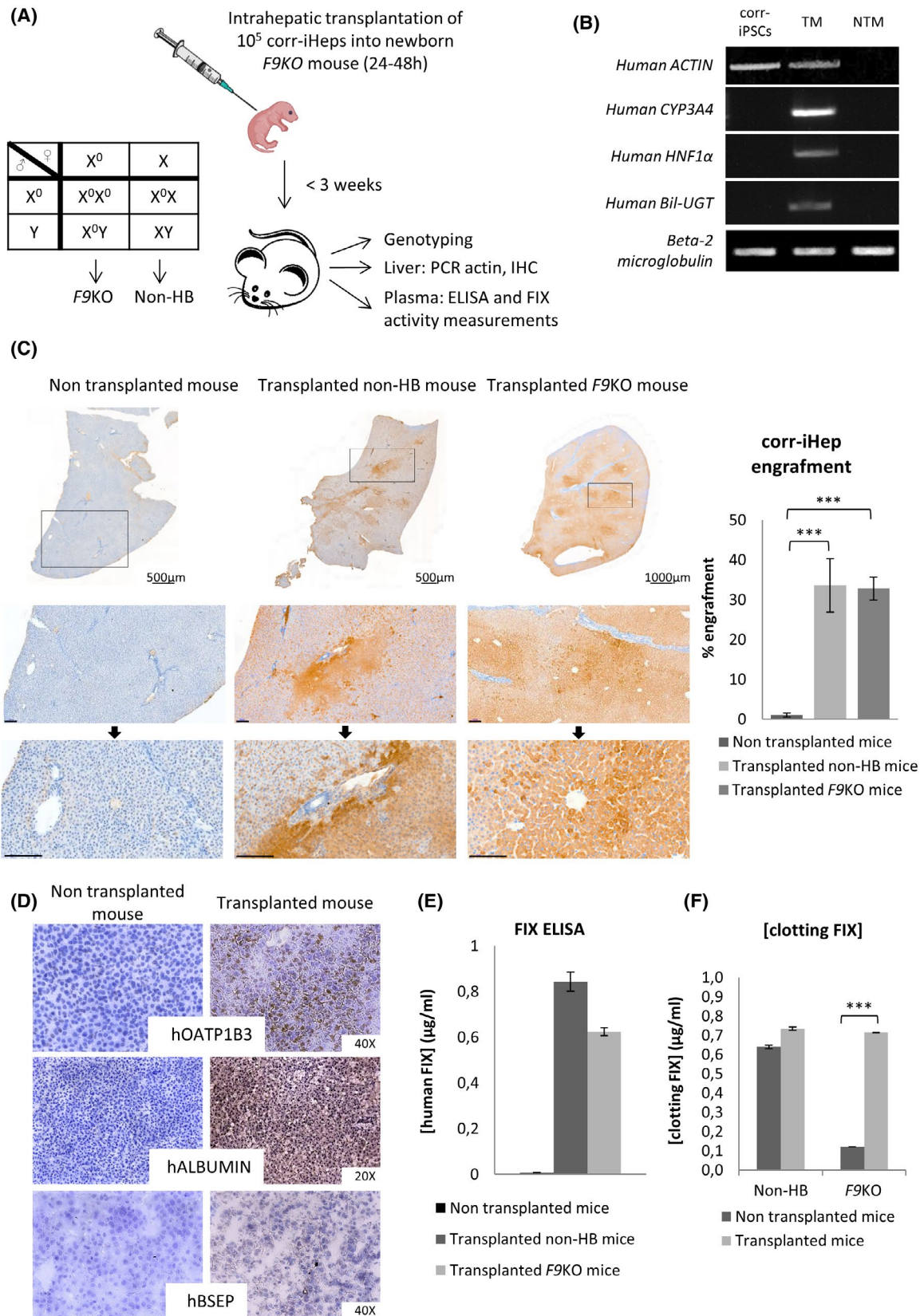mbinant FIX used as a control. This result confirmed the improvement in the hepatocyte differentiation protocol after organoid formation and prompted us to assess FIX activity. Chromogenic analyses of FIX activity in the cell supernatant at day 30 confirmed the absence of activity of the endogenous FIX produced by HB-iHeps due to the g.31280 G>A mutation. By contrast, we detected FIX activity in the supernatant of corr-iHeps, due to
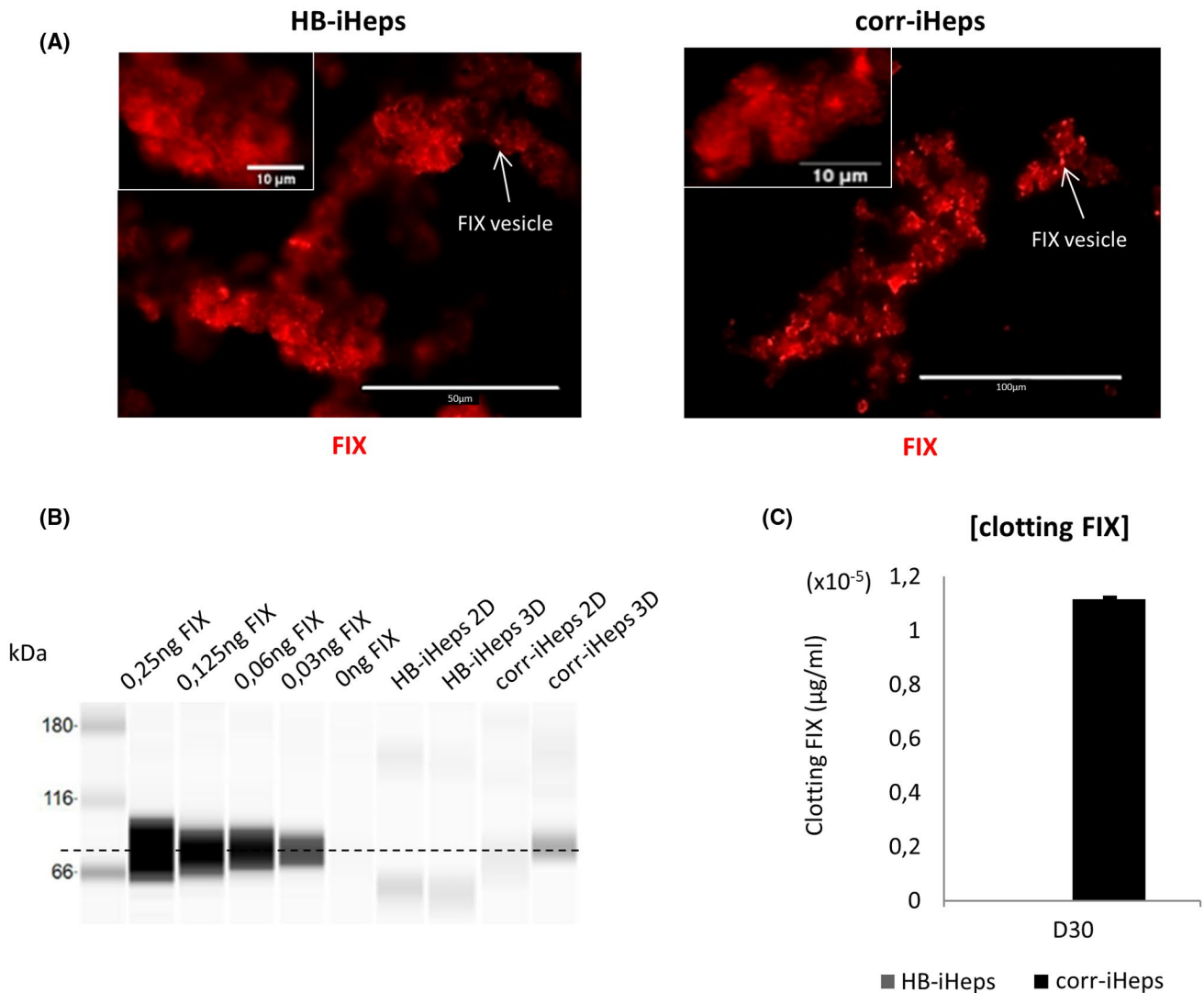
FIGURE 5 Phenotypic rescue of corr-iHeps in vitro. (A) FIX immunostaining of HB-iHeps and corr-iHeps at day 25 on cryosections of organoids embedded in OCT. (B) WES analysis of FIX extracted from HB-iHeps and corr-iHeps at day 30. Decreasing concentrations of recombinant FIX were used as controls. (C) Concentrations of clotting FIX determined by chromogenic assay in both HB-iHeps and corr-iHeps at day 30 of 3D differentiation

FIGURE 6 Genetic correction rescues the HB phenotype in vivo. (A) Schematic representation of the strategy for in vivo validation of the cell/gene therapy approach. (B) PCR analyses confirm the presence of human DNA in the liver of transplanted animals. PCR primers recognizing both mouse and human β-2 microglobulin gene were used for internal control. (C) Representative immunohistochemistry images of mouse liver paraffin sections using human-specific OTC antibody. Scale bars of zoomed sections represent 100 µm. The percentage engraftment was determined using ImageJ. Results are expressed as mean ± SD (n = 5). Statistical significance was determined using the Student t test; ***p < 0.001. (D) Immunohistochemistry images of mouse liver paraffin sections using human-specific antibodies. (E) Human FIX secretion into mouse plasma was determined by a human FIX-specific ELISA assay. No human FIX has been detected in non-transplanted mice, and similar levels of FIX antigen were measured in both non-HB and $F9$KO transplanted mice. Results are expressed as mean ± SD (n = 3). (F) FIX clotting activity was determined in mouse plasma using a chromogenic test. Results are expressed as mean ± SD (n = 3 for non-HB and n = 2 for $F9$KO). Statistical significance was determined using the Student t test; ***p < 0.001

(A)

Intrahepatic transplantation of 10^5 corr-iHeps into newborn *F9*KO mouse (24-48h)

♂\♀	X^0	X
X^0	X^0X^0	X^0X
Y	X^0Y	XY

↓ *F9*KO ↓ Non-HB

< 3 weeks

→ Genotyping
→ Liver: PCR actin, IHC
→ Plasma: ELISA and FIX activity measurements

(B)

corr-iPSCs TM NTM

Human ACTIN

Human CYP3A4

Human HNF1α

Human Bil-UGT

Beta-2 microglobulin

(C)

Non transplanted mouse   Transplanted non-HB mouse   Transplanted *F9*KO mouse

500μm   500μm   1000μm

corr-iHep engrafment

% engrafment

***
***

■ Non transplanted mice
■ Transplanted non-HB mice
■ Transplanted *F9*KO mice

(D) Non transplanted mouse   Transplanted mouse

hOATP1B3   40X

hALBUMIN   20X

hBSEP   40X

(E)

FIX ELISA

[human FIX] (μg/ml)

■ Non transplanted mice
■ Transplanted non-HB mice
■ Transplanted *F9*KO mice

(F)

[clotting FIX]

[clotting FIX] (μg/ml)

***

Non-HB   *F9*KO

■ Non transplanted mice
■ Transplanted mice

production of the FIX encoded by the therapeutic cassette (Figure 5C). This result confirmed the improved maturation of hepatocytes differentiated in organoids but also the therapeutic potential of our approach, which we next tested in vivo.

Genetic correction rescues the HB phenotype in vivo

We then assessed the phenotypic correction in vivo using a mouse model of HB (*F9*KO). Corrected cells

at day 11 of differentiation were transplanted into the liver of newborn mice and the animals were sacrificed after 2 weeks, before maturation of the immune system (Figure 6A). The mice were then genotyped and their plasma and livers analyzed. Because the identification of newborn mice was not possible at the time of transplantation, we transplanted the entire litter obtained by mating heterozygous females and hemophilic males during each experiment. Nonquantitative PCR performed on DNA extracted from the mouse livers revealed the presence of human DNA in the liver of the transplanted mice (Figure 6B). The engraftment and repopulation of the mouse livers were visualized using human-specific antibodies (Figure 6C,D). We evaluated cell engraftment at 33% in both non-HB and *F9*KO mice (Figure 6C and Figure S4A). Circulating human FIX was measured using ELISA in the plasma of transplanted mice and showed similar levels of the protein in all animals (Figure 6E). This ELISA is specific to human FIX and does not cross react with murine FIX, as shown by the absence of hFIX detected in non-transplanted animals (Figure 6E and Figure S4B). Finally, a chromogenic analysis of FIX activity was performed on transplanted mouse plasmas. We first confirmed the phenotype of the *F9*KO mouse model showing 40% of wild-type (WT) FIX activity in heterozygous $F9^{+/-}$ mice and 1.7% of WT FIX activity in *F9*KO animals (Figure S4C). After transplantation, we determined a significant increase in clotting activity in *F9*KO animals, reaching a level similar to that seen in non-HB mice (Figure 6F). It should be noted that the activity/antigen ratio of human FIX was close to 1 in the transplanted *F9*KO mice, indicating good maturation of the FIX in the producer cells.

DISCUSSION

We report the generation of HB-iPSCs and HB-iHeps from a patient with severe HB (FIX c < 1%; IXAg 67%) carrying a g.31280 G>A mutation. This led to the production of an inactive form of the FIX protein, which enabled us to decipher both protein production and activity in vitro.

CRISPR/Cas9 technology has been widely used to correct numerous genetic defects under two different approaches: (1) CRISPR/Cas9-based point correction to replace the mutated base pair and restore the native sequence, or (2) a more universal correction approach with full-length cDNA knocked into the genome. Because many variants of HB have been observed to date, and are still being discovered,[27] we adopted the second approach and targeted correction cassette insertion into AAVS1, a safe-harbor site that has been used in many studies.[13] We were able to confirm insertion of the therapeutic cassette at the targeted site and its absence from the principal off-target sites.

Although other studies have previously reported the hepatocyte differentiation of CRISPR/Cas9-corrected HB-iPSCs,[12,13,15,16] none of them achieved a detailed in vitro characterization of these cells to be used as an in vitro model of the disease. We therefore studied both mature hepatocyte markers but also deciphered the production and post-translational modification of FIX by differentiated cells. Both HB-iHeps and corr-iHeps expressed hepatocyte markers, such as *CYP3A4/3A7/2B6*, *Bil-UGT*, HNF4α and albumin, and show evidence of epithelial polarity, lipid and glycogen storage, and albumin secretion, all suggestive of mature features of stem cell–derived hepatocytes in vitro. However, we observed a significant difference in the size of the protein produced by iHeps using a classic 2D culture system when compared with recombinant and plasmatic FIX. This difference was partly due to the absence of γ-carboxylation of the GLA-rich domain of the protein. Indeed, FIX is synthesized by hepatocytes in the liver as a pre-prozymogen of 52 kDa containing a pro-peptide that is recognized by a vitamin K–dependent carboxylase (γ-glutamyl carboxylase),[28] which converts 12 N-terminal glutamic acid residues of the GLA domain into gamma-carboxyglutamic acid (Gla), leading to a change in its conformation crucial for FIX activity.[29] These post-translational modifications were also problematic during recombinant FIX production in vitro and led to a low protein production yield until complex co-expression systems of FIX and the necessary modification enzymes have been set up.[30] We therefore developed a differentiation strategy that includes a cell aggregation step, to improve the cell–cell interactions known to promote functional PSC-derived hepatic cell maturation.[31]

Both HB-iHep and corr-iHep organoids showed an improvement in cell differentiation when compared with the 2D protocol; this was reflected by higher albumin production together with the collapse of AFP secretion, the expression of mature polarized hepatocyte markers (CYP3A4/2B6, SRB1, CK8, CX32, MDR3, and BSEP), and metabolic functions from phase 1 to 3. They expressed a FIX protein that, unlike 2D differentiated cells, had the same size as the recombinant or plasmatic protein, confirming post-translational modifications of FIX and hence an improvement in cell maturation under 3D conditions.

Compared with other studies that evaluated the global clotting activity of the cell supernatant, which is usually poorly concentrated in clotting FIX, we directly measured the concentration of clotting FIX in the corr-iHep supernatant. The low clotting activity detected in vitro could be explained by potential degradation of the protein, as large vitamin K–dependent proteins such as FIX contain high levels of carbohydrates and are rapidly degraded by proteases, or by dilution of the protein in the supernatant volume. Indeed, several methods can be used to evaluate FIX activity in vitro, but the sensitivity

of certain assays is very low and affected by numerous parameters such as cell density, incubation time, and culture medium.[32] This difficult evaluation of clotting activity has recently been reported by others who showed broad variations in the measurement of FIX activity levels, depending on the assay used.[33] However, in the case of severe HB, just a minor improvement in FIX levels or repopulation efficiency should be sufficient to achieve therapeutic effectiveness.

We then evaluated the efficacy of a therapeutic approach in a mouse model of HB. Because we did not have access to an immunodeficient hemophilic mouse model, we decided to transplant the corr-iHeps into newborn *F9*KO mice via the intrahepatic route. Indeed, the liver continues to grow after birth until it reaches its adult size.[34] This proliferative stimulus, most often triggered by a partial hepatectomy in adults, which is problematic in the case of HB, can improve hepatocyte engraftment and proliferation. Moreover, because it takes about 2–3 weeks after birth for the mouse immune system to become effective,[35] resulting in the rejection of a xenogenic transplant, we sacrificed the transplanted animals after 2 weeks. Transplanted cell engraftment was confirmed by PCR and evaluated to reach more than 30% by immunohistochemistry. Similar levels of human FIX antigen were detected in the plasma of both non-HB (WT) and *F9*KO transplanted mice. Finally, the FIX clotting activity measured in *F9*KO mice transplanted with corr-iHeps confirmed correction of the hemophilic phenotype. Our study revealed a normal morphology of transplanted livers with no sign of hyperplasia or transplanted cell overgrowth, but long-term analysis in another mouse model will be necessary.

To conclude, the development of an improved differentiation protocol involving 3D culture has allowed the differentiation of hiPSCs into fully functional hepatocytes able to secrete mature FIX with clotting activity. This enabled the establishment of an in vitro human HB model that is suitable to study FIX production and activity, which might offer a predictive tool that is more accurate than animal models and could be used in therapeutic approaches such as drug screening. In vivo, our approach could provide a therapeutic alternative to patients who are not eligible for gene therapy, or to pediatric patients in whom hepatocyte transplantation might prove more appropriate than the injection of non-integrative AAV vectors that could be lost during liver growth.

CONFLICT OF INTEREST
Nothing to report.

AUTHOR CONTRIBUTIONS
Study design: Anne Dubart-Kupperschmitt, Eléanor Luce, and Anne Weber *Data analysis:* Anne Dubart-Kupperschmitt and Eléanor Luce *Data interpretation:* Anne Dubart-Kupperschmitt, Eléanor Luce, and Olivier Christophe. *Manuscript draft:* Anne Dubart-Kupperschmitt, Eléanor Luce, and Olivier Christophe. *Experiments:* Eléanor Luce, Clara Steichen, Olivier Christophe, Tuan Huy Nguyen, Jean-Marie Heslan, Mickaël Allouche, Antonietta Messina, and Thierry Lambert. *Funding obtainment:* Anne Dubart-Kupperschmitt and Anne Weber.

ORCID
Eléanor Luce https://orcid.org/0000-0002-8938-8405
Clara Steichen https://orcid.org/0000-0003-1201-4904
Antonietta Messina https://orcid.org/0000-0002-5610-973X
Thierry Lambert https://orcid.org/0000-0001-6391-5839
Olivier Christophe https://orcid.org/0000-0002-9080-6336
Anne Dubart-Kupperschmitt https://orcid.org/0000-0002-9326-4413

REFERENCES
1. Zhao Y, Weyand AC, Shavit JA. Novel treatments for hemophilia through rebalancing of the coagulation cascade. Pediatr Blood Cancer. 2021;68:e28934.
2. Perrin GQ, Herzog RW, Markusic DM. Update on clinical gene therapy for hemophilia. Blood. 2019;133:407–14.
3. Simioni P, Tormene D, Tognin G, Gavasso S, Bulato C, Iacobelli NP, et al. X-linked thrombophilia with a mutant factor IX (Factor IX Padua). N Engl J Med. 2009;361:1671–5.
4. Harris JE, Balk JL, Mobley CM, Heyne K. The liver that cured Christmas: case report of orthotopic liver transplant in a patient with hemophilia B. Case Rep Transplant. 2020;2020:7873803.
5. Weber A, Mahieu-Caputo D, Hadchouel M, Franco D. Hepatocyte transplantation: studies in preclinical models. J Inherit Metab Dis. 2006;29:436–41.
6. Elaut G, Henkens T, Papeleu P, Snykers S, Vinken M, Vanhaecke T, et al. Molecular mechanisms underlying the dedifferentiation process of isolated hepatocytes and their cultures. Curr Drug Metab. 2006;7:629–60.
7. Broutier L, Andersson-Rolf A, Hindley CJ, Boj SF, Clevers H, Koo B-K, et al. Culture and establishment of self-renewing

human and mouse adult liver and pancreas 3D organoids and their genetic manipulation. Nat Protoc. 2016;11:1724–43.

8. Takahashi K, Tanabe K, Ohnuki M, Narita M, Ichisaka T, Tomoda K, et al. Induction of pluripotent stem cells from adult human fibroblasts by defined factors. Cell. 2007;131:861–72.

9. Yamanaka S. Pluripotent stem cell-based cell therapy—promise and challenges. Cell Stem Cell. 2020;27:523–31.

10. Si-Tayeb K, Noto FK, Nagaoka M, Li J, Battle MA, Duris C, et al. Highly efficient generation of human hepatocyte-like cells from induced pluripotent stem cells. Hepatology. 2010;51:297–305.

11. Touboul T, Hannan NRF, Corbineau S, Martinez A, Martinet C, Branchereau S, et al. Generation of functional hepatocytes from human embryonic stem cells under chemically defined conditions that recapitulate liver development. Hepatology. 2010;51:1754–65.

12. He Q, Wang H-H, Cheng T, Yuan W-P, Ma Y-P, Jiang Y-P, et al. Genetic correction and hepatic differentiation of hemophilia B-specific human induced pluripotent stem cells. Chin Med Sci J. 2017;32:135–44.

13. Lyu C, Shen J, Wang R, Gu H, Zhang J, Xue F, et al. Targeted genome engineering in human induced pluripotent stem cells from patients with hemophilia B using the CRISPR-Cas9 system. Stem Cell Res Ther. 2018;9:92.

14. Martorell L, Luce E, Vazquez JL, Richaud-Patin Y, Jimenez-Delgado S, Corrales I, et al. Advanced cell-based modeling of the royal disease: characterization of the mutated F9 mRNA. J Thromb Haemost. 2017;15:2188–97.

15. Morishige S, Mizuno S, Ozawa H, Nakamura T, Mazahery A, Nomura K, et al. CRISPR/Cas9-mediated gene correction in hemophilia B patient-derived iPSCs. Int J Hematol. 2020;111:225–33.

16. Ramaswamy S, Tonnu N, Menon T, Lewis BM, Green KT, Wampler D, et al. Autologous and heterologous cell therapy for hemophilia B toward functional restoration of factor IX. Cell Rep. 2018;23:1565–80.

17. Sadelain M, Papapetrou EP, Bushman FD. Safe harbours for the integration of new DNA in the human genome. Nat Rev Cancer. 2011;12:51–8.

18. Baxter M, Withey S, Harrison S, Segeritz C-P, Zhang F, Atkinson-Dell R, et al. Phenotypic and functional analyses show stem cell-derived hepatocyte-like cells better mimic fetal rather than adult hepatocytes. J Hepatol. 2015;62:581–9.

19. Messina A, Morelli S, Forgacs G, Barbieri G, Drioli E, De Bartolo L. Self-assembly of tissue spheroids on polymeric membranes. J Tissue Eng Regen Med. 2017;11:2090–103.

20. Lin HF, Maeda N, Smithies O, Straight DL, Stafford DW. A co-agulation factor IX-deficient mouse model for human hemophilia B. Blood. 1997;90:3962–6.

21. Dianat N, Dubois-Pot-Schneider H, Steichen C, Desterke C, Leclerc P, Raveux A, et al. Generation of functional cholangiocyte-like cells from human pluripotent stem cells and HepaRG cells. Hepatology. 2014;60:700–14.

22. Touboul T, Chen S, To CC, Mora-Castilla S, Sabatini K, Tukey RH, et al. Stage-specific regulation of the WNT/β-catenin pathway enhances differentiation of hESCs into hepatocytes. J Hepatol. 2016;64:1315–26.

23. Bone HK, Nelson AS, Goldring CE, Tosh D, Welham MJ. A novel chemically directed route for the generation of definitive endoderm from human embryonic stem cells based on inhibition of GSK-3. J Cell Sci. 2011;124:1992–2000.

24. Suttie JW. Synthesis of vitamin K-dependent proteins. FASEB J. 1993;7:445–52.

25. Subramanian K, Owens DJ, Raju R, Firpo M, O'Brien TD, Verfaillie CM, et al. Spheroid culture for enhanced differentiation of human embryonic stem cells to hepatocyte-like cells. Stem Cells Dev. 2014;23:124–31.

26. Qin J, Chang M, Wang S, Liu Z, Zhu W, Wang YI, et al. Connexin 32-mediated cell-cell communication is essential for hepatic differentiation from human embryonic stem cells. Sci Rep. 2016;6:37388.

27. Zhang X, Wang G, Chen K, Zhang C, Qin X, Zhang Y, et al. Identification of five novel variants of haemophilia B in 32 patients in Shanxi province, China. Haemoph Off J World Fed Hemoph. 2020;26:e217–9.

28. Brandstetter H, Bauer M, Huber R, Lollar P, Bode W. X-ray structure of clotting factor IXa: active site and module structure related to Xase activity and hemophilia B. Proc Natl Acad Sci. 1995;92:9796–800.

29. Stenflo J. Contributions of Gla and EGF-like domains to the function of vitamin K-dependent coagulation factors. Crit Rev Eukaryot Gene Expr. 1999;9:59–88.

30. Liu J, Jonebring A, Hagström J, Nyström A-C, Lövgren A. Improved expression of recombinant human factor IX by co-expression of GGCX. Protein J. 2014;33:174–83.

31. Blau BJ, Miki T. The role of cellular interactions in the induction of hepatocyte polarity and functional maturation in stem cell-derived hepatic cells. Differentiation. 2019;106:42–8.

32. Lengler J, Coulibaly S, Gruber B, Ilk R, Mayrhofer J, Scheiflinger F, et al. Development of an in vitro biopotency assay for an AAV8 hemophilia B gene therapy vector suitable for clinical product release. Mol Ther Methods Clin Dev. 2020;17:581–8.

33. Nederlof A, Kitchen S, Meijer P, Cnossen M, Ali Pour N, Kershaw G, et al. Performance of FIX extended half-life product measurements in external quality control assessment programmes. J Thromb Haemost. 2020;18:1874–83.

34. Grijalva J, Vakili K. Neonatal liver physiology. Semin Pediatr Surg. 2013;22:185–9.

35. Holsapple MP, West LJ, Landreth KS. Species comparison of anatomical and functional immune system development. Birth Defects Res B Devs Reprod Toxicol. 2003;68:321–34.

36. Arganda-Carreras I, Fernández-González R, Muñoz-Barrutia A, Ortiz-De-Solorzano C. 3D reconstruction of histological sections: application to mammary gland tissue. Microsc Res Tech. 2010;73:1019–29.

SUPPORTING INFORMATION

Additional supporting information may be found in the online version of the article at the publisher's website.